Article

Not peer-reviewed version

A Novel Hemocyte-Derived Peptide and Its Possible Roles in Immune Response of Ciona intestinalis Type A

Shin Matsubara * , Rin Iguchi , Michio Ogasawara , Hiroya Nakamura , Tatsuki R. Kataoka , Akira Shiraishi , Tomohiro Osugi , Tsuyoshi Kawada , Honoo Satake

Posted Date: 20 December 2023

doi: 10.20944/preprints202312.1565.v1

Keywords: ascidian; Ciona; hemocyte; stomach; pharynx; peptide; immune response

Article

A Novel Hemocyte-Derived Peptide and Its Possible Roles in Immune Response of *Ciona intestinalis* Type A

Shin Matsubara [1,*], Rin Iguchi [2], Michio Ogasawara [2], Hiroya Nakamura [3], Tatsuki R Kataoka [3], Akira Shiraishi [1], Tomohiro Osugi [1], Tsuyoshi Kawada [1] and Honoo Satake [1]

[1] Bioorganic Research Institute, Suntory Foundation for Life Sciences, 8-1-1 Seikadai, Seika-cho, Soraku-gun, Kyoto 619-0284, Japan; shiraishi@sunbor.or.jp (A.S.); osugi@sunbor.or.jp (T.O.); kawada@sunbor.or.jp (T.K.); satake@sunbor.or.jp (H.S.)

[2] Department of Biology, Graduate School of Science, Chiba University, 1-33 Yayoi-cho, Inage-ku, Chiba 263-8522, Japan; iguchirin@chiba-u.jp (R.I.); ogasawara@faculty.chiba-u.jp (M.O.)

[3] Department of Pathology, Iwate Medical University, 2-1-1 Idaidori, Yahaba-cho, Shiwa-gun, Iwate 028-3695, Japan; nkhiroy@iwate-med.ac.jp (H.N.); trkata@iwate-med.ac.jp (T.R.K.)

* Correspondence: matsubara@sunbor.or.jp; Tel.: +81-7022881395

Abstract: A wide variety of bioactive peptides have been identified in the central nervous system and several peripheral tissues in the ascidian *Ciona intestinalis* type A (*Ciona robusta*). However, hemocyte endocrine peptides have yet to be explored. Here, we report a novel 14-amino acid peptide, CiEMa, that is predominant in the granular hemocytes and unilocular refractile granulocytes of *Ciona*. RNA-seq and qRT-PCR revealed the high *CiEma* expression in the adult pharynx and stomach. Immunohistochemistry further revealed the highly concentrated CiEMa in the hemolymph of the pharynx and epithelial cells of the stomach, suggesting biological roles in the immune response. Notably, bacterial lipopolysaccharide stimulation of isolated hemocytes for 1-4 hours resulted in increased CiEMa secretion. Furthermore, CiEMa-stimulated pharynx exhibited mRNA upregulation of the growth factor (*Fgf3/7/10/22*), vanadium binding proteins (*CiVanabin1* and *CiVanabin3*), and forkhead and homeobox transcription factors (*Foxl2*, *Hox3*, and *Dbx*), but not antimicrobial peptides (*CrPap-a* and *CrMam-a*) or immune-related genes (*Tgfbtun3*, *Tnfa*, and *Il17-2*). Collectively, these results suggest that CiEMa plays roles in signal transduction involving tissue development or repair in the immune response, rather than in the direct regulation of immune-response genes. The present study identified a novel *Ciona* hemocyte peptide, CiEMa, providing insights into the molecular and functional diversity of the immune response in chordates.

Keywords: ascidian; *Ciona*; hemocyte; stomach; pharynx; peptide; immune response

1. Introduction

An immune system against invading pathogenic microbes is essential for all living organisms. The adaptive immune system is believed to be a slow but specific system acquired in jawed vertebrates; in contrast, the innate immune system is a rapid and primary defensive system against a broad spectrum of pathogens, not only in vertebrates but also in invertebrates. The significant success of the adaptive immune system hypothesizes the reduction of the molecular variation of the innate immune system in vertebrates [1]. On the other hand, some invertebrates have evolved a wide variety of recognition and effector molecules via genome-wide expansion or diversification of innate immune-related genes in a species-specific manner [2–5].

Ascidians are marine invertebrates belonging to the phylum Urochordata; these organisms represent the closest living relatives to vertebrates [6,7]. Given its phylogenetically important position in the superphylum Chordata, the cosmopolitan species *Ciona intestinalis* type A (synonymous with *Ciona robusta*) has been studied as a model organism in various fields of evolution including genomics, developmental biology, endocrinology, and immunology [8–16]. The availability of

 doi:10.20944/preprints202312.1565.v1

genomic information and a growing body of RNA-seq data has facilitated studies of the molecular basis of the immune response in *Ciona* and the conservation of those in vertebrates [12–19].

The primary immune defense in ascidians is employed by the circulating hemocytes, the pharynx, and the alimentary canal [12–15]. Several genes involved in diverse pathogen recognition including lectins, complements, and Toll-like receptors, have so far been demonstrated to be expressed in the *Ciona* hemocytes and pharynx [11–15]. In a previous study, thirty-four *Ciona* hemocyte-specific genes were identified, of which three were immune-related homologs of vertebrates (e.g., complement 6-like) [20]. However, twenty-three of the genes were either unknown or *Ciona*-specific, twelve of which were polypeptides (shorter than 100 residues). Additionally, a genome-wide search for discovering antimicrobial peptides (AMPs) identified numerous functionally uncharacterized peptides, suggesting the presence of *Ciona*-specific mechanisms of immune response [21]. Nevertheless, large parts of these *Ciona*-specific peptides and their signaling in immune response remain to be elucidated.

In vertebrates, some bioactive peptides are known to regulate immune cells, while others show antimicrobial activities [22,23]. We have previously identified various neuropeptides in the *Ciona* neural complex [24] and demonstrated the reproductive function of several orthologous peptides to vertebrates [24–29]. In addition, we recently identified a novel *Ciona*-specific 51-amino acid peptide, PEP51, and verified its possible roles in the activation of caspase in the ovary [30]. In *Ciona* hemocytes, several AMPs, including CrMAM-A, CrPAP-A, and others have been reported [21,31,32]. Furthermore, a 73-amino acid *Ciona* chemo-attractive peptide (CrCP) derived from alternative transcript upregulated in hemocytes by bacterial lipopolysaccharide (LPS) stimulation [33,34]. However, the endogenous roles of many other *Ciona*-specific hemocyte peptides remain largely unknown.

In the present study, we identified a novel 14-amino acid peptide, CiEMa, from *Ciona* hemocytes and demonstrated that CiEMa was predominantly expressed in granular hemocytes (GHs) and unilocular refractile granulocytes (URGs). LPS challenge induced CiEMa secretion from the hemocytes, which then acted on the pharynx and thereby upregulated several gene expressions including *Fgf3/7/10/22*, *CiVanabins*, and transcription factors. These suggest that CiEMa plays key roles underlying the immune response in *Ciona* hemocytes, and provide evolutionary insights into immune-response signaling in chordates.

2. Results

We previously performed peptidomic analysis on *Ciona* neural complexes and identified more than 30 neuropeptides [24]. In the neuropeptide-enriched gel-filtration fraction, MALDI-TOF mass spectrometry (MS) analysis identified several known neuropeptides (CiLF6, CiTKI, CiYFL1, and CiNTLP6) as well as an unknown major peak with an *m/z* of 1628.877, suggesting the presence of novel neuropeptide (Figure 1A). MS/MS analyses of this peak in the neural complex and ovary showed MS/MS patterns similar to those of the synthetic peptide of NERKGAEPQFPPEM-amide. The MS-tag analyses for the neural complex detected most of theoretical fragment peaks (Figure 1B) and confirmed the amino acid sequence, that is encoded by the KY21.Chr12.349 gene (Figure 2A).

Preprints (www.preprints.org) | NOT PEER-REVIEWED | Posted: 20 December 2023 doi:10.20944/preprints202312.1565.v1

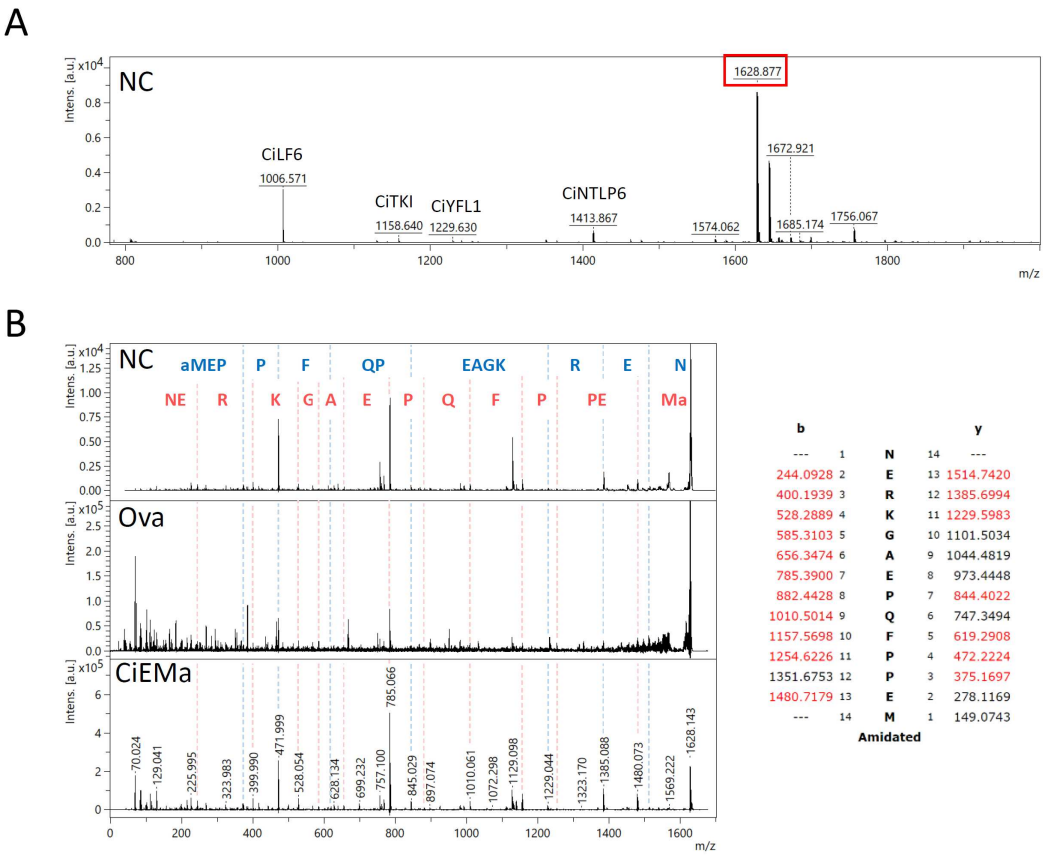

Figure 1. Identification of a novel peptide, CiEMa from the *Ciona* neural complex and ovary. (A) MALDI-TOF analysis of the peptide-enriched fraction of the neural complex. Several annotated peptides, including CiLF6, CiTKI, CiYFL1, and CiNTLP6, were detected. A predominant peak with an *m*/*z* of 1628.877 was also observed. (B, left) Tandem MS analyses on the precursor ion of 1628.5 in the neural complex and ovary. Most of the MS/MS peaks of the neural complex and ovary were identical to those of a synthetic peptide (NERKGAEPQFPPEM-amide). (B, right) MS-tag analyses, using a mass list of fragment ions of the neural complex, identified theoretical b- and y-ions (shown in red). The experiments were performed independently at least three times.

No BLASTP hits against the non-redundant protein database indicated that this peptide is *Ciona*-specific. Further *in silico* analyses using SignalP and DeepLoc for KY21.Chr12.349 predicted that the N-terminal sequences would be a signal peptide and the processed peptide is secreted (Figure 2B and C). The aforementioned sequence of mature peptide is likely to be produced via an unusual cleavage between Trp and Asn at the N-terminus and Gly and Asp at the C-terminus, followed by amidation of the C-terminal Gly (Figure 2A). We designated this novel peptide CiEMa based on the C-terminal sequence.

Preprints (www.preprints.org) | NOT PEER-REVIEWED | Posted: 20 December 2023 doi:10.20944/preprints202312.1565.v1

A

>KY21.Chr12.349
MDRKIVFALLLLMSVQVSMAFHWNERKGAEPQFPPEMGDEIAADA
ERLMRKAAKDHWSNKMAKDVIWWEQ

B

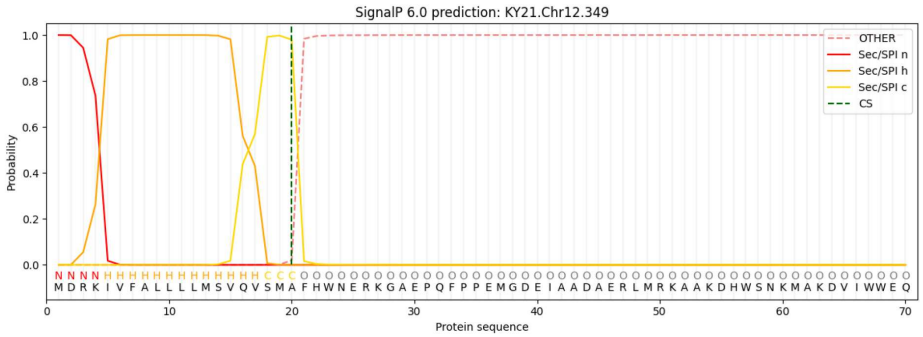

C

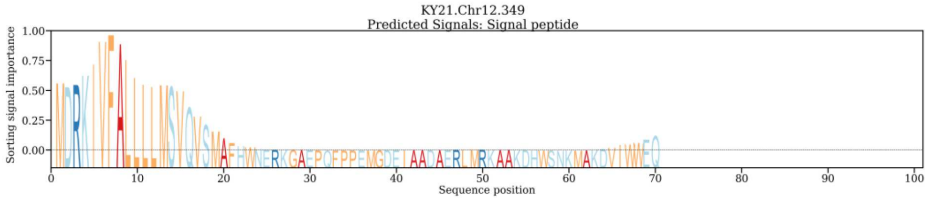

Localizations	Signals	Cytoplasm	Nucleus	Extracellular	Cell membrane
Extracellular	Signal peptide	0.116	0.025	**0.958**	0.038
Mitochondrion	**Plastid**	**Endoplasmic reticulum**	**Lysosome/ Vacuole**	**Golgi apparatus**	**Peroxisome**
0.044	0.004	0.072	0.163	0.122	0.002

Figure 2. *In silico* analyses of the precursor sequence of CiEMa. (A) The translated sequence of the *CiEma* gene from the Ghost database is shown. The predicted N-terminal signal sequence is marked in grey, and the mature peptide identified in Figure 1 is shown in red. (B) The N-terminal signal sequence was predicted using SignalP 6.0. The peptide bond between Ala20 and Phe21 is suggested to be the cleavage site. (C) Subcellular localization of CiEMa was predicted using DeepLoc 2.0. The N-terminal sequence was predicted to serve as a signal peptide (upper panel), and CiEMa was predicted to be secreted into the extracellular region (lower panel).

We then investigated the localization of CiEMa in the ovary and neural complex. Interestingly, *in situ* hybridization (ISH) of the ovary revealed that the *CiEma* mRNA was expressed specifically in interfollicular hemocyte cells, but not in the ovarian follicle cells (Figure 3A). Consistent with the ISH results, immunohistochemistry (IHC) demonstrated that the CiEMa peptide was expressed predominantly in hemocytes (Figure 3A). These results confirmed the specificity of the ISH probes and anti-CiEMa antibodies. Similarly, in the neural complex, CiEMa was not expressed in the neural cells in the cerebral ganglion or neural gland, but rather in a few hemocytes around the neural gland or in the ciliated funnel (Figure 3B). These results strongly suggested that specific CiEMa expression in circulating hemocytes and distinct biological roles from neuropeptides or ovarian peptide hormones.

Preprints (www.preprints.org) | NOT PEER-REVIEWED | Posted: 20 December 2023 doi:10.20944/preprints202312.1565.v1

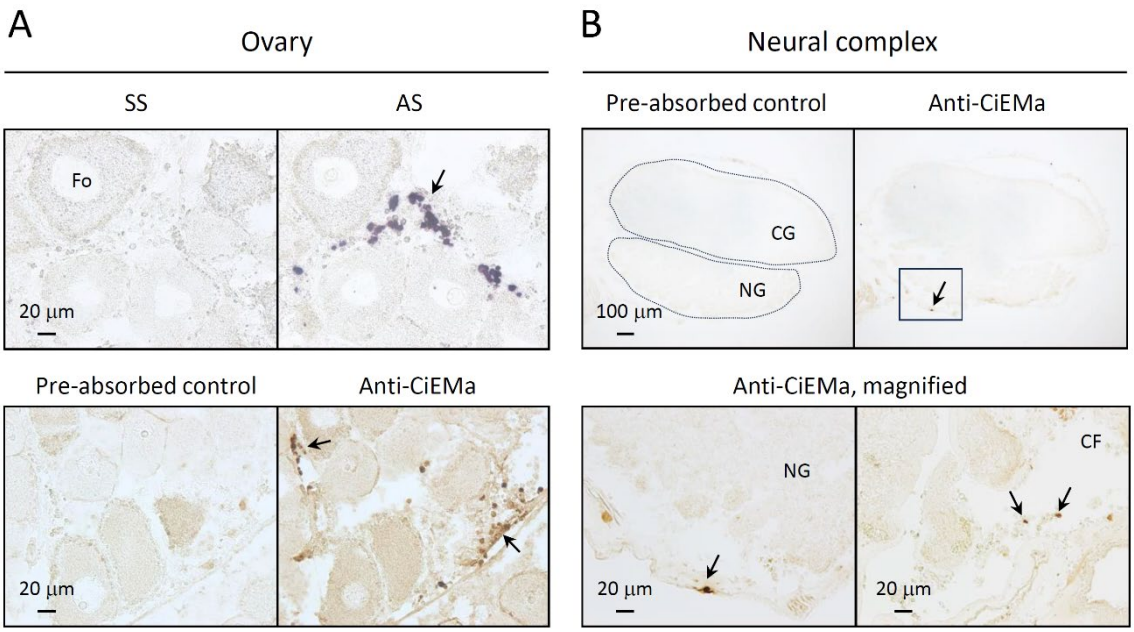

Figure 3. Localization of CiEMa in the ovary and neural complex. (A) *In situ* hybridization (ISH, upper panels) and immunohistochemistry (IHC, lower panels) of CiEMa in the ovary. 4% PFA- and Bouin's-fixed ovaries were used for the ISH and IHC, respectively. Signals were detected using the DIG-NBT/BCIP system for ISH and the ABC system for IHC, respectively. For ISH, the sense probe was used as a negative control; specific signals were observed in the antisense probe (arrow). For IHC, the pre-absorbed antibody was used as a negative control; specific signals were observed in the anti-CiEMa antibody (arrow). Fo, follicles. The scale bar represents 20 μm. (B) IHC of CiEMa in the neural complex. (Upper) Low-magnification images indicated no signals in the cerebral ganglion (CG) and neural gland (NG). The boxed area in the upper panel is magnified and shown below. (Lower) High-magnification images indicate specific expression in the hemocytes around the NG and in the ciliated funnel (CF) (arrows). Scale bars in the upper and lower panels represent 100 μm and 20 μm, respectively. Localization was confirmed using two or three independent tissues.

Subsequently, we isolated *Ciona* hemocytes from the heart and investigated CiEMa expression. Seven to eight types of morphologically distinct *Ciona* hemocytes have been reported and classified into two groups: agranular and granular hemocytes [13]. Immunocytochemistry (ICC) demonstrated that no signals were detected in four types of agranular hemocytes (lymphocyte-like cells (LLCs), signet ring cells (SRCs), hyaline amoebocytes (HAs), or compartment cells (CCs)). On the other hand, in granular cells, weak and strong signals were observed in GHs and URGs, respectively, but not in morula cells (MCs) (Figure 4). These results are not inconsistent with the hemocyte expression in the ovary and neural complex (Figures 1 and 3). *Ciona* hemocytes are known to be important for the primary immune defense, and GHs and URGs have been shown to express several immune-related genes [13–15], suggesting that CiEMa plays a role in the immune system by circulating throughout the body.

Preprints (www.preprints.org) | NOT PEER-REVIEWED | Posted: 20 December 2023 doi:10.20944/preprints202312.1565.v1

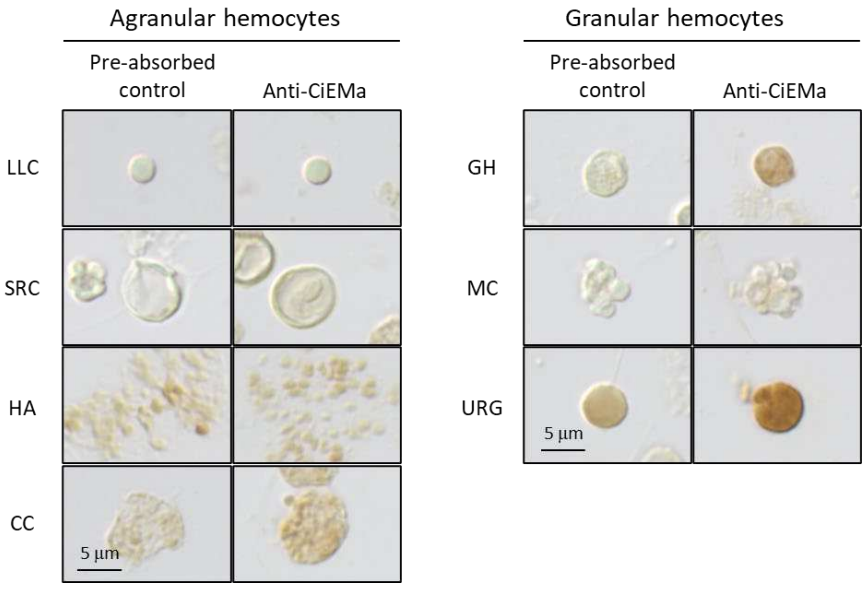

Figure 4. Localization of CiEMa in *Ciona* hemocytes. *Ciona* hemocytes were isolated by rupturing the heart, collected in an anticoagulant-containing buffer, dried on the slides, and subjected to immunocytochemistry (ICC). Blocking, immunoreaction, and signal detection were performed as IHC. The *Ciona* hemocytes were distinguished by their morphology. LLC, lymphocyte-like cell; SRC, signet ring cell; HA, hyaline amoebocyte; CC, compartment cell; GH, granular hemocyte; MC, morula cell; URG, unilocular refractile granulocyte. The scale bar represents 5 μm. Expression was confirmed in three independent experiments.

Thus, we referred to the *CiEma* expression during early embryo development and found that *CiEma* was first expressed at around the juvenile stage [35]. We then examined expression in two-week-old juveniles by whole-mount ISH (WISH). As in Figure 3A, specific signals were observed using antisense probes (Figure 5A-D), and not with the control (sense) probes (Figure 5E-H). In accordance with Figures 3 and 4, the *CiEma* mRNA expression in juveniles was observed predominantly in the hemocytes distributed to the neural complex (Figure 5B and F), pharynx (Figure 5C and G), and stomach (Figure 5D and H). Moreover, distinct broad signals were also observed in the stomach (Figure 5D and H).

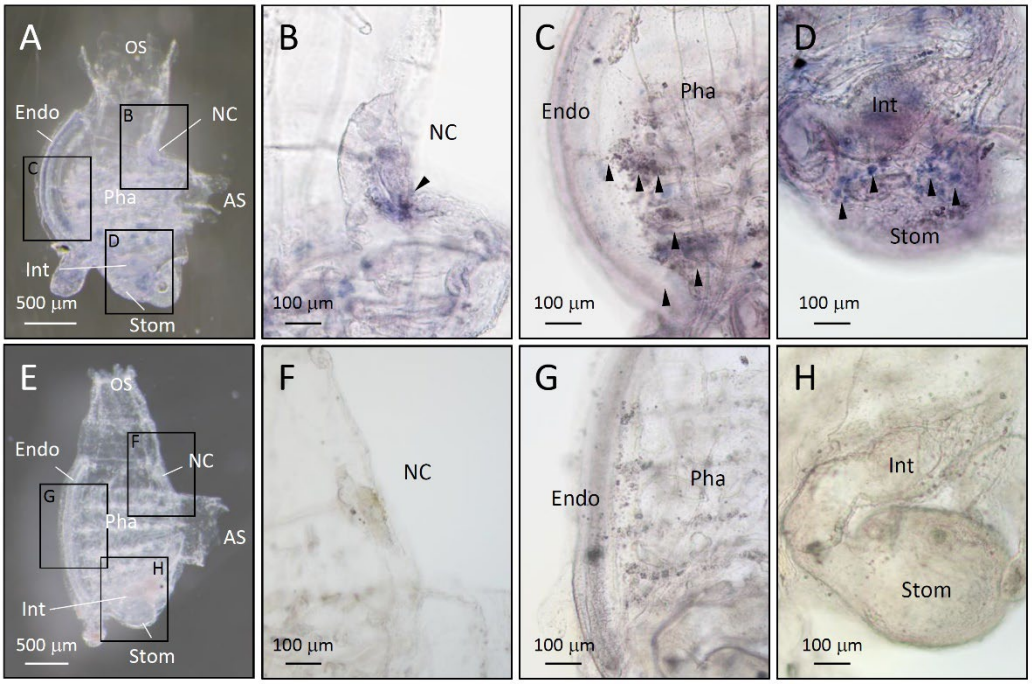

Preprints (www.preprints.org) | NOT PEER-REVIEWED | Posted: 20 December 2023 doi:10.20944/preprints202312.1565.v1

Figure 5. Localization of CiEMa in *Ciona* juveniles. Two-week-old juveniles were used for WISH. Panels (A) and (E) show overviews of *Ciona* juveniles at low magnification following hybridization with antisense (A) and sense (E) probes. The indicated areas in (A) and (E) are shown at high magnification in (B-D) and (F-H), respectively. The hemocyte-specific signals (arrowheads) were observed in the neural complex (B and F), pharynx (C and G), and stomach (D and H). The stomach also showed broad signals (D and H). OS, oral siphon; AS, atrial siphon; NC, neural complex; Pha, pharynx; Stom, stomach; Int, intestine; Endo, endostyle. Scale bars represent 500 μm in (A) and (E) and 100 μm in (B-D) and (F-H), respectively. Expression was confirmed using approximately ten juveniles.

We previously obtained transcriptomic data from 11 samples of 9 adult tissues (Figure 6A) [10], leading to the detection of high *CiEma* expression in the pharynx and stomach but low in the neural complex and ovary (Figure 6B). The tissue distribution and statistically significant expression in the pharynx were confirmed by qRT-PCR (Figure 6B). Furthermore, IHC confirmed the specific expression of CiEMa in the hemocytes of the pharynx and stomach (Figure 7). Of note, some parts of the body fluid (hemolymph) showed strong signals (Figure 7A, arrowheads), indicating the secretion of CiEMa by hemocytes. The epithelial cells of the inner fold also showed strong signals that were not observed in the outer fold of the stomach. Furthermore, both the apical and basolateral sides of the epicardium were strongly stained (Figure 7B), suggesting multiple roles of CiEMa in the *Ciona* stomach. Combined with the fact that the *Ciona* pharynx and stomach are most exposed to the microbiome in the marine environment and are the major organs of immunity [13], these results suggested that CiEMa plays a role in the immune response to microbes.

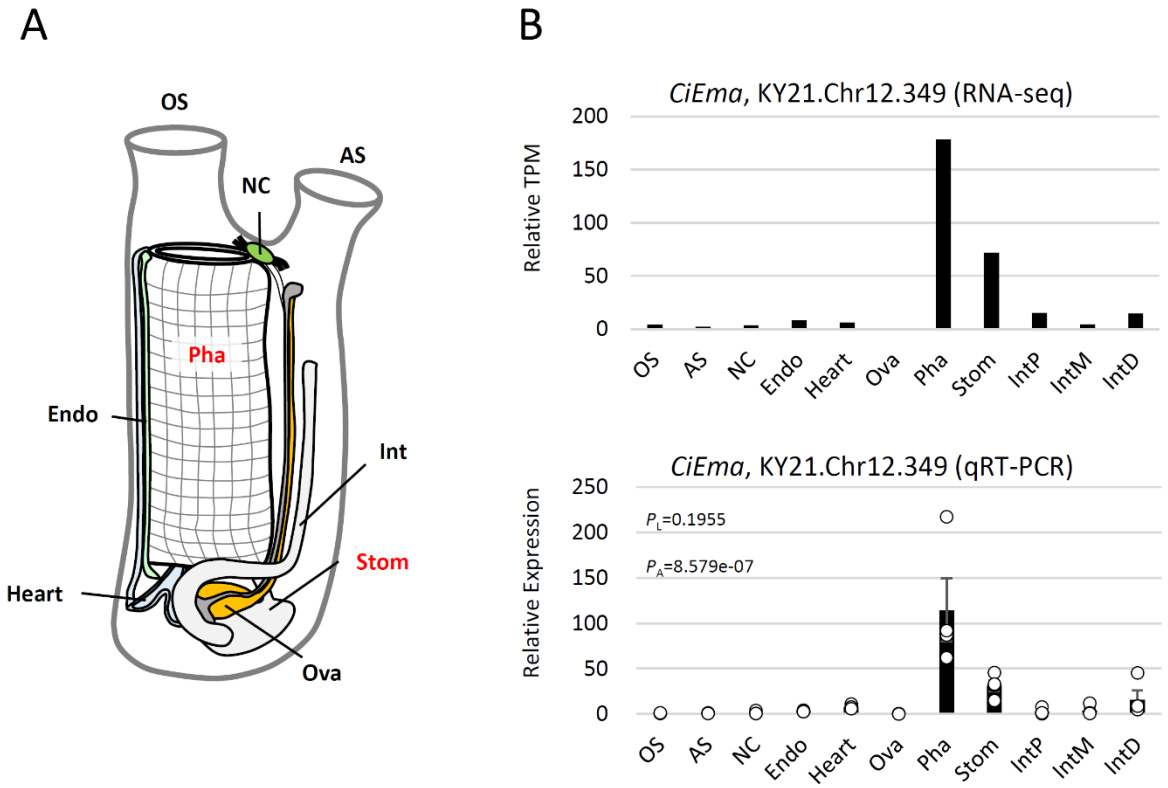

Figure 6. Tissue distribution of *CiEMa* mRNA in adult *Ciona*. (A) A schematic illustration of adult *Ciona* tissues (modified from Osugi et al., 2020 [36]). OS, oral siphon; AS, atrial siphon; NC, neural complex; Pha, pharynx; Stom, stomach; Int, intestine; Endo, endostyle. (B) The previous RNA-seq data [10] for adult *Ciona* tissues were analyzed (upper). qRT-PCR analyssis confirmed the tissue distribution of *CiEma* (lower). Relative expression to the reference gene (KY21.Chr10.446) [10] was indicated. Data are shown as the mean ± SEM with data points. Four independent data sets were

Preprints (www.preprints.org) | NOT PEER-REVIEWED | Posted: 20 December 2023 doi:10.20944/preprints202312.1565.v1

analyzed using the Levene (P_L=0.1955) test followed by one-way ANOVA (P_A=8.579e-07). IntP, proximal intestine; IntM, middle intestine; IntD, distal intestine.

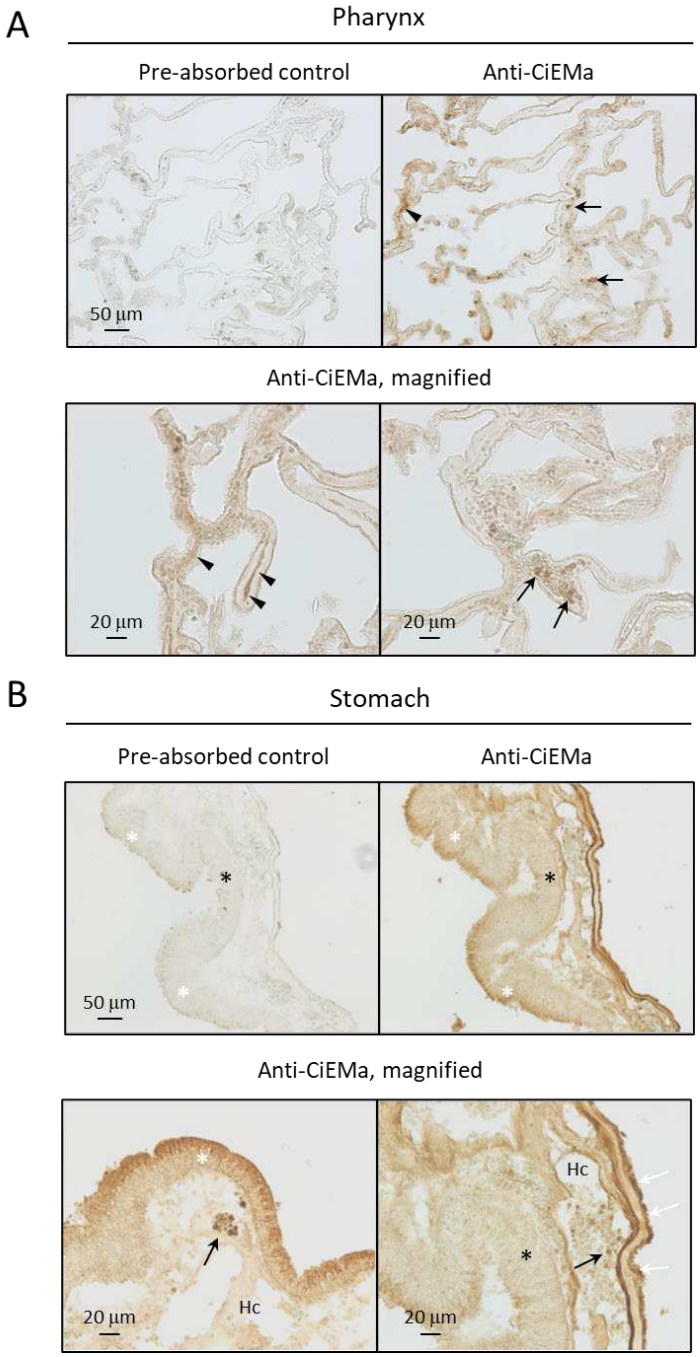

Figure 7. Localization of CiEMa in the pharynx and stomach. The Bouin's-fixed pharynx (A) and stomach (B) were used for IHC. Serial sections were probed with either the pre-absorbed negative control or the anti-CiEMa antibody. (A) Signal was detected in the hemocytes (black arrows) and hemolymph (arrowheads). (B) In addition to the hemocytes (black arrows), strong signals were detected in the epithelial cells of the inner fold (white asterisk) but not in the outer fold (black asterisk). Strong signal was observed on both the apical and basolateral sides of the epicardium (white arrows). Hc, hemocoel. Scale bars in the upper and lower panels represent 50 µm and 20 µm, respectively. Expression was confirmed in two different tissues.

Subsequently, we investigated the effects of a bacterial LPS as a non-self antigen on CiEMa expression. We treated isolated hemocytes with LPS and examined the mRNA expression and secretion of CiEMa. Although some AMP genes have been reported to be upregulated in 1 hour after

Preprints (www.preprints.org) | NOT PEER-REVIEWED | Posted: 20 December 2023 doi:10.20944/preprints202312.1565.v1

LPS challenge [21], no significant change was observed in *CiEma* mRNA levels following LPS stimulation (Figure 8A). Next, CiEMa secretion was examined by dot blot analyses using supernatants of hemocytes that had been incubated in the absence or presence of LPS. In contrast to the case with mRNA, stronger signals were observed at every time point following LPS stimulation (1, 2, and 4 hours) (Figure 8B left). Quantification using Fiji software demonstrated that those signals were increased significantly 2.7-, 1.9-, and 2.4-fold at 1, 2, and 4 hours, respectively (Figure 8B right). The original images and quantification file are provided as Figure S1 and Table S1. These results indicated that secretion of CiEMa by hemocytes increases in response to stimulation with LPS, a non-self antigen.

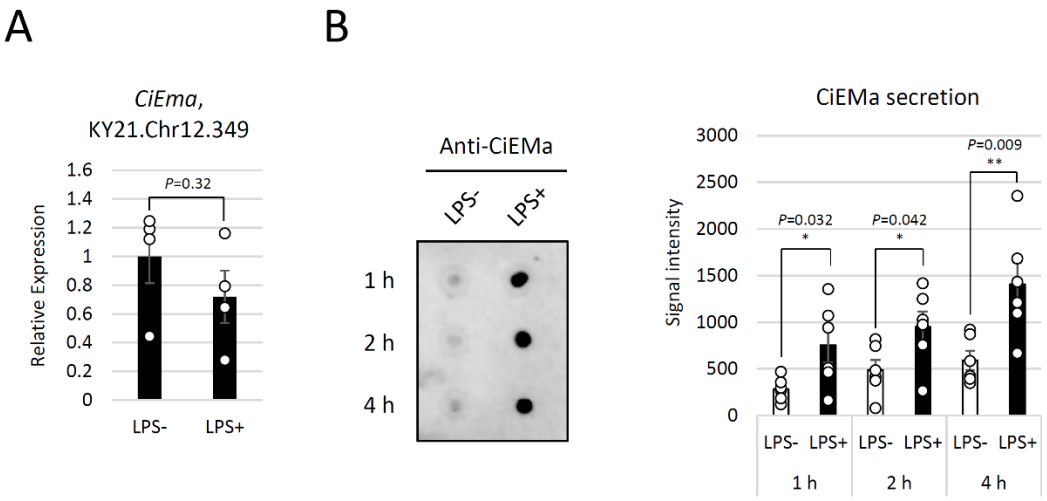

Figure 8. Induction of CiEMa secretion by LPS challenge. (A) Hemocytes isolated from adults were incubated with or without LPS for 1 hour, and *CiEma* expression was examined by qRT-PCR. Relative expression to the reference gene (KY21.Chr9.158 (KH.C9.410)) [21] was indicated. Four independent data sets were analyzed by Student's *t*-test (*P*=0.32) and are presented as the mean ± SEM with data points. (B) Hemocytes were incubated with or without LPS for 1, 2, and 4 hours, and CiEMa secretion was examined by dot blot. Signals were quantified using Fiji software. Data are shown as the mean ± SEM with data points. Six independent data sets were analyzed by Student's *t*-test *, *P*=0.032, 0.042, and **, 0.009 for 1, 2, and 4 hours, respectively.

Given the strong signals in the hemolymph (Figure 7A), the pharynx is presumed to be the primary target of CiEMa. Therefore, we isolated the pharynx, stimulated it with 1 μM CiEMa for 0, 1, 2, 4, and 8 hours, and subjected them to RNA-seq. The resulting reads, mapping rates, and NCBI SRA accessions are summarized in Table 1. The expression level (TPM, transcripts per million) of each gene was calculated and provided in Table S2. The expression patterns following CiEMa stimulation were confirmed by qRT-PCR (Figure 9). Unexpectedly, none of the known *Ciona* AMP genes including *CrPap-a*, *CrMam-a*, KY21.Chr7.694 (KH.C7.94), and KY21.Chr2.890 (KH.S908.1) exhibited significant changes in response to CiEMa (Figure 9). The time-dependent change of the immune-related genes in the *Ciona* pharynx during LPS challenge has been reported [13]. Among the genes, *Tgfbtun3* was significantly downregulated, while *Mmp2/9/13* was upregulated 8 hours after CiEMa stimulation. The cytokine expressions (*Tnfa* and *Il17-2*) showed no significant change during CiEMa stimulation. Of particular interest is that a few signaling genes including *Ghsr-like* and the growth factor, *Fgf3/7/10/22*, and several forkhead and homeobox transcription factors (*Foxl2*, *Hox3*, *Dbx*, and *Prrx*) were upregulated by CiEMa. Moreover, vanadium-binding proteins (*CiVanabin1* and *CiVanabin3*) were also significantly induced (Figure 9). Consequently, these results strongly suggest that CiEMa plays a role in cell growth and/or tissue repair via regulation of the growth factor and transcription factors, rather than direct regulation of immune-response genes including AMPs and cytokines. Taken together, these results verified the novel cascade of immune response mediated by

Preprints (www.preprints.org) | NOT PEER-REVIEWED | Posted: 20 December 2023 doi:10.20944/preprints202312.1565.v1

CiEMa: the non-self antigen LPS acts on GHs and URGs to induce CiEMa secretion, which leads in turn to the upregulation of various genes in the pharynx (Figure 10).

Table 1. RNA-seq of the CiEMa-stimulated *Ciona* pharynx.

Sample	Total reads	% mapped	Accession
Pha_CiEMa_0h	70,659,570	84.93	SRR26963725
Pha_CiEMa_1h	80,794,444	85.50	SRR26963724
Pha_CiEMa_2h	84,126,938	85.08	SRR26963723
Pha_CiEMa_4h	84,462,016	84.30	SRR26963722
Pha_CiEMa_8h	109,996,394	87.07	SRR26963721

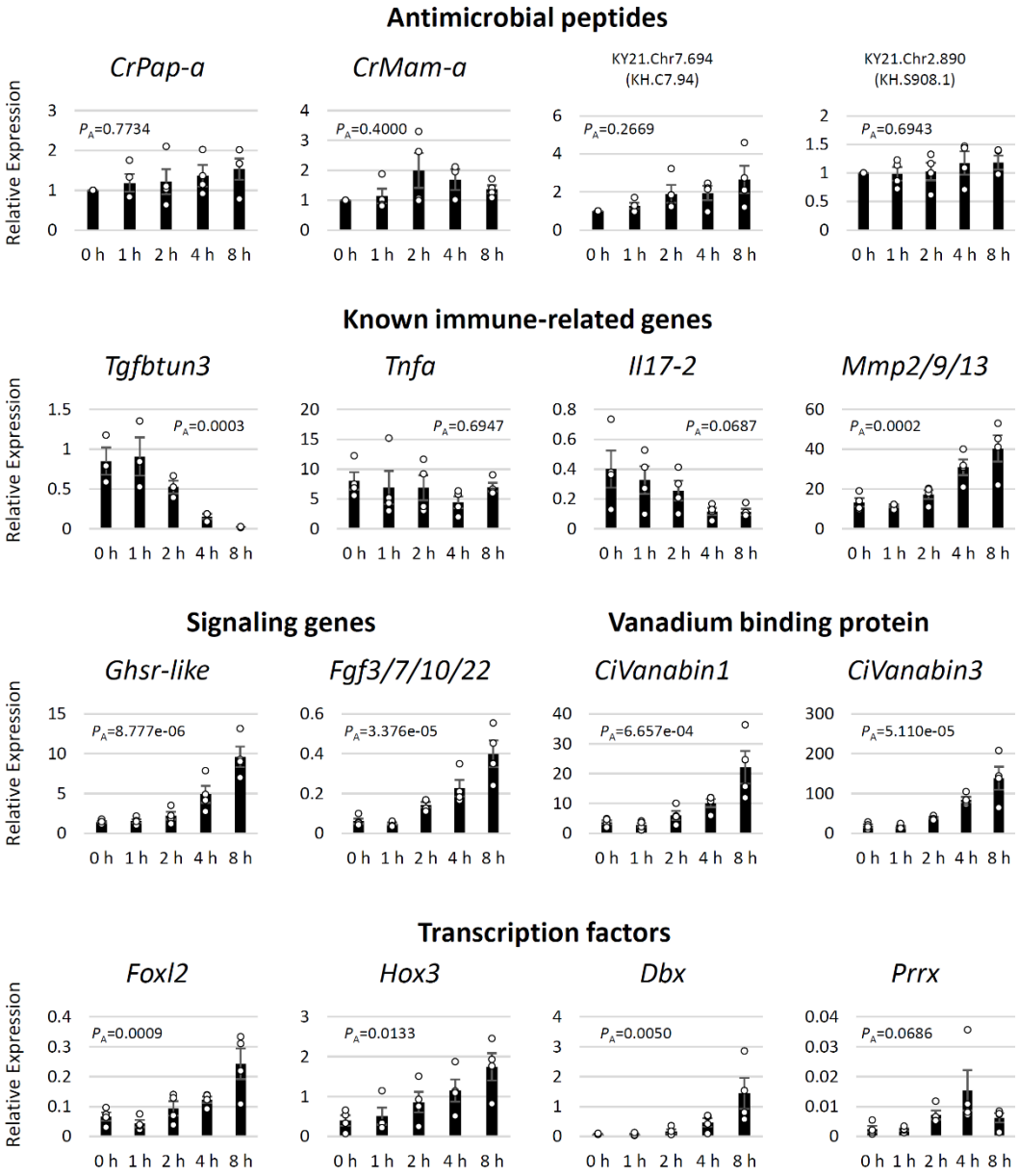

Figure 9. Gene expression change in the CiEMa-stimulated pharynx. Differentially expressed genes screened on RNA-seq data were confirmed by qRT-PCR. Expression is shown relative to the reference gene (KY21.Chr2.148), which was identified by RNA-seq to be constantly expressed. Data are shown as the mean ± SEM with data points. Three to four independent data sets were analyzed by one-way ANOVA and P_A values are indicated in each graph. The expression value of AMP genes for the 0

Preprints (www.preprints.org) | NOT PEER-REVIEWED | Posted: 20 December 2023 doi:10.20944/preprints202312.1565.v1

hours was set to 1, given that the expression levels before CiEMa stimulation varied among the sample sets.

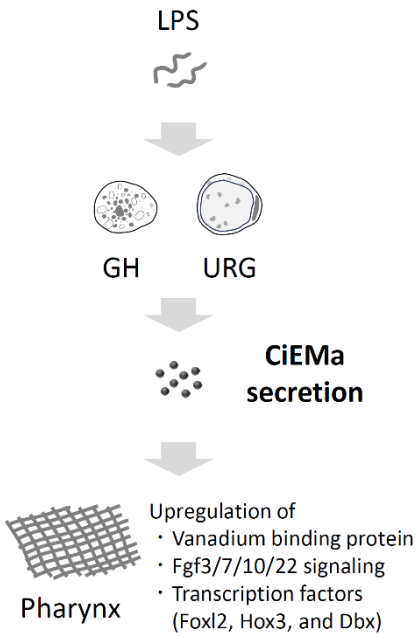

Figure 10. Schematic diagram summarizing the proposed model. CiEMa secretion from the hemocytes, namely GHs and URGs, is induced in response to bacterial lipopolysaccharide (LPS) as non-self antigen. The CiEMa in turn affects the pharynx (indicated by the cross-hatched surface) and upregulates the expression of genes regarding vanabins, signaling molecules, and transcription factors. GH, granular hemocyte; URG, unilocular refractile granulocyte.

3. Discussion

In the past two decades, along with the assembly of the genome and cDNA libraries, various *Ciona* hemocyte-derived transcripts have been identified and attracted attention to the evolutionary lineage of the innate immune system [17,20,37,38]. Based on genome sequencing data and homology searching, several immune-related genes including complement components, Toll-like receptors, lectins, and cytokines have been characterized as counterparts of their vertebrate homologs [11,13,17,39]. The easy isolation and fractionation methods of *Ciona* hemocytes, and the application of LPS challenge to ascidian individuals, enabled us to investigate the immune system of ascidians and underscored the usefulness of *Ciona* as an evolutionary model organism of the innate immune system [13]. In contrast to the homologous molecules to vertebrates, *Ciona*-specific molecules have been less investigated. In this study, we identified a novel hemocyte-derived peptide, CiEMa, and demonstrated the possible roles in the immune response of the *Ciona* pharynx.

We first identified CiEMa from the neural complex and ovary (Figure 1) and found to be expressed in the specific hemocytes (Figures 3 and 4). *In silico* prediction of CiEMa being secreted (Figure 2) was substantiated by immunoreactivities in hemolymph (Figure 7A) and dot blot analyses using supernatants of hemocyte incubates (Figure 8B). Consistent with the fact that hemocytes initially emerge at the 1st ascidian stages of juveniles [40], our WISH analyses confirmed the hemocyte expression in two-week-old juveniles (Figure 5). The overall tissue distribution was maintained in the adult ascidians in that predominant expression in the hemocytes in the pharynx and epithelial expression in the stomach (Figures 6 and 7). Given that the pharynx, stomach, and hemocytes are important sites for primary immune defense [13], CiEMa is likely to play roles in the immune response.

In the stomach, the epithelial cells, especially those of the inner fold, are known to express several genes involved in pinocytosis and phagocytosis [41]. Particularly, the strong expression of CiEMa in the bottom of inner fold cells was similar to that of the phagocytosis-related cell surface receptor,

 doi:10.20944/preprints202312.1565.v1

Mrc1 (mannose receptor C-type 1). The endosome-like expression of CiEMa in the stomach epithelium supports a possible role in the uptake of large particles and/or small nutrients. Moreover, the variable region-containing chitin-binding protein A (VCBP-A) has been shown to accumulate in identical large (endosome-like) vacuoles in the inner fold [42], raising the possibility that CiEMa supports the opsonizing function of VCBP-A. In contrast, CiEMa was unlikely to be involved in the digestion, given that it is not expressed in the outer-fold cells where is enriched for pancreatic enzymes [43]. Thus, CiEMa may play distinct roles in epithelial cells of the stomach and in hemocytes.

CiEMa showed the most predominant expression in both juvenile and adult hemocytes (Figures 3-7). Of interest, the CiEMa signal was not observed in all hemocytes but only in some clusters of GH and URG hemocytes, suggesting specific roles in these particular cell types (Figures 3A, 4, 5B-D, and 7). GHs and URGs have been reported to express various immune-related genes including cytokines, phenoloxidases, and complements [13]. Although *CiEma* mRNA expression did not change following LPS stimulation, increased CiEMa secretion from isolated hemocytes was observed (Figure 8). Similar expressions have been reported for some *Ciona* cytokines and relevant signaling molecules including CiTGFb, CiTNFa and CiIL17s in the clustered hemocytes of LPS-challenged ascidians [44–46], supporting the view that CiEMa plays a cytokine-like role as a signal transduction molecule in response to non-self antigens.

Most of the known hemocyte-derived signaling molecules are cytokines [13–15]. The three *CiIl17* genes have been shown to upregulate following LPS challenge [45]. The *CiTnfa* also has been shown to be induced in hemocytes at 4 hours after LPS injection [44]. Of particular interest is that CiEMa did not alter the *Tnfa* expression, and downregulated the *Il17-2* (Figure 9), suggesting that CiEMa plays roles distinct from those of typical cytokines. Moreover, none of the examined AMP genes were affected by CiEMa stimulation (Figure 9), suggesting that CiEMa is likely to be involved in other functions rather than direct regulation of immune processes.

In general, FGF signaling, homeobox proteins, and forkhead-box proteins are key regulators of cell proliferation, differentiation, and embryonic development in both vertebrates and invertebrates. *Ciona* FGF3/7/10/22 is important for notochord development in tailbud stage embryos [47]. In contrast, disruption of *CiHox3* did not affect the normal expression of neuronal markers in the swimming larva [48]. Although no other functional insights of signaling genes and transcription factors in Figure 9 in adult tissues have been reported, upregulation in 4 or 8 hours after CiEMa stimulation implies possible roles in tissue development or repair via cell proliferation and differentiation. In addition, five vanadium-binding protein genes, *CiVanabins* have been identified [49], and two of which, *CiVanabin1* and *CiVanabin3*, were upregulated by CiEMa. In *Ascidia sydneiensis samea*, vanabins have been shown to be expressed in SRCs, a type of agranular hemocyte [50,51]. In *C. intestinalis* type A, SRCs have been shown to express the AMP CrMAM-A and the galectins (CrGal-a and CrGal-b) [13,52,53]. These findings raise the possibility that vanadium accumulation contributes to the immune response in ascidians.

Most vertebrates have acquired sophisticated adaptive immune systems employing major histocompatibility complexes, T-cell receptors, and immunoglobulins. These changes are hypothesized to have led to decreases in the number of components of the innate immune system [1]. In contrast, in invertebrates, various innate immune molecules have evolved such as lectins [54], AMPs [55], and cytokines [56]. Additionally, *Ciona* has developed a variety of species-specific peptides including CrCP [33,34], PEP51 [30], and CiEMa. As observed in CiEMa, a signaling molecule produced by atypical processing at Trp or Asp, may contribute to the diversification of signal transduction in the ascidian immune response. Combined with the fact that such unconventional processing of peptides has also been reported in other invertebrates [57–60], the observation of numerous functionally uncharacterized peptides in *Ciona* suggests that these factors serve as novel cytokine-like or immune-related signaling peptides. Although further functional analyses are required, the current study identified a novel hemocyte-derived peptide and proposed possible roles in the immune response in *Ciona* (Figure 10), providing evolutionary insights into the innate immune systems of chordates.

 doi:10.20944/preprints202312.1565.v1

4. Materials and Methods

4.1. Animals

Adult ascidians (*Ciona intestinalis* type A, *Ciona robusta*) were cultivated at the Maizuru Fisheries Research Station of Kyoto University or the Misaki Marine Biological Station of the University of Tokyo, where the animals were maintained at 18 °C in sterile artificial sea water (ASW). Two-week-old juveniles were produced by artificial insemination, as reported previously [43].

4.2. Peptide extraction and detection by mass spectrometry

Peptides from adult *Ciona* tissues were extracted and purified as previously [24]. In brief, 20 neural complexes and 5 ovaries were homogenized in liquid nitrogen. Peptides were obtained using an extraction buffer (methanol/water/acetic acid, 90:9:1) supplemented with PMSF. Following incubation for 30 min at room temperature, the buffer was exchanged for 30% acetonitrile containing 0.1% trifluoroacetic acid (TFA) using a Speed-Vac lyophilizer. The peptide-enriched fraction from the neural complex then was separated by Superdex 30 Increase 10/300 GL gel filtration column chromatography (10 × 300 mm, GE Healthcare, Buckinghamshire, UK). The eluent was dried using a Speed-Vac, and the precipitates (peptides) were dissolved in 0.1% TFA. Separately, the predicted mature peptide (NERKGAEPQFPPEM-amide) was synthesized and purified commercially (PH Japan Co., Ltd., Hiroshima, Japan). The peptides were analyzed using a rapifleX MALDI-TOF spectrometer (Bruker Daltonics, Bremen, Germany). The MS/MS spectrum data for the peptide extracts from the neural complex were analyzed using MS-Tag (https://prospector.ucsf.edu/prospector/cgi-bin/msform.cgi?form=mstagstandard) for confirmation of the amino acid sequences. Analyses were conducted as more than three independent experiments.

4.3. In silico analyses of CiEMa

The predicted amino acid sequence of the KY21.Chr12.349 gene was obtained from the *Ciona* ghost database (http://ghost.zool.kyoto-u.ac.jp/default_ht.html) [61]. The signal peptide was predicted using SignalP 6.0 (https://services.healthtech.dtu.dk/services/SignalP-6.0/). Subcellular localization was predicted using DeepLoc 2.0 (https://services.healthtech.dtu.dk/services/DeepLoc-2.0/).

4.4. In situ hybridization (ISH)

mRNA localization in the *Ciona* ovary was performed as previously [27]. In brief, cDNA fragments of CiEMa (KY21.Chr12.349) were obtained from *Ciona* ovaries using a primer pair (ACGCATTCCAGACAAATCTCAA and GCTCCAATGATCCTTTGCAGC) and cloned into the pCR™4-TOPO Vector (Thermo Fisher Scientific, Waltham, MA, USA). The sequence-confirmed vector was linearized using NotI or PmeI and used for digoxigenin (DIG)-labeling (Roche, Basel, Switzerland). Adult *Ciona* ovaries were fixed overnight at 4 °C with 4% paraformaldehyde (PFA) in ASW; the fixative was exchanged with 30% sucrose, and the tissue was embedded in super cryoembedding medium (SCEM). 10-µm cryosections were prepared and subjected to ISH as previously [27]. Specifically, hybridization was performed at 60 °C for 16 hours in a hybridization buffer (50% formamide, 10 mM Tris-HCl, 1 mM EDTA, 0.6 M NaCl, 10% dextran sulfate, 1×Denhardt's solution, 0.25% SDS, and 0.2 mg/mL yeast transfer RNA). After washing and blocking of the slides, signals were developed using alkaline phosphatase-conjugated anti-DIG antibody (Roche, 1:5000) and NBT/BCIP (Nacalai Tesque, Inc., Kyoto, Japan) system. Three independent ovaries were examined. For the whole-mount experiment, two-week-old *Ciona* juveniles were fixed with 4% PFA and whole-mount ISH (WISH) was performed using the "InSitu Chip", as previously described [20].

 doi:10.20944/preprints202312.1565.v1

4.5. Antibody generation and purification

The CiEMa-antigen peptide (KLH-CNERKGAEPQFPPEM-amide) was synthesized and purified commercially (PH Japan Co., Ltd.). A CiEMa-specific arabbit antibody was raised by immunization of two animals (Eurofins Genomics, Tokyo, Japan). The anti-CiEMa antibodies were affinity purified using KLH-free antigen peptides (Eurofins Genomics). The purified antibodies were stocked at 0.29 mg/mL in a solution of 50% glycerol in phosphate-buffered saline (PBS) and maintained at -30 °C.

4.6. Immunohistochemistry (IHC)

Adult *Ciona* tissues (ovary, neural complex, pharynx, and stomach) were fixed overnight at 4 °C with Bouin's solution; following exchange of the fixative for 30% sucrose in PBS, the ovaries were embedded in SCEM and cryosectioned at 10-μm. IHC was performed as previously [27]. The affinity-purified anti-CiEMa antibody, diluted 1:150-300 in Can Get Signal immunostain Solution A (Toyobo, Osaka, Japan), was used as the primary antibody. To generate the pre-absorbed antibody for a negative control, the anti-CiEMa antibodies were preincubated with an excess (approximately 80 μg) of KLH-free CiEMa. Immunoreactivity was developed using an Avidin-Biotin Complex (ABC) kit (Vector Laboratories, Burlingame, CA, USA) according to the instructions. Two independent tissues were examined.

4.7. Hemocyte collection and immunocytochemistry (ICC)

Adult *Ciona* hemocytes were collected by rupturing the heart, and the cells were subjected to centrifugation (1000 ×g, 5 min, 18 °C). Both the supernatant and pellet were used in subsequent experiments. The supernatant was filtered and used as hemolymph. The cell pellet was suspended in an anticoagulant buffer (11 mM KCl, 43 mM Tris-HCl, 0.4 M NaCl, 10 mM EDTA) [62] and used as hemocytes. Aliquots of the hemocyte suspension were placed on slides allowed to dry at room temperature, then subjected to ICC. In brief, the slides were further dried for 1 hour at 37 °C before fixing for 10 min with 4% PFA in PBS. Subsequent steps of blocking, immunoreaction, and signal detection were performed as for IHC. The experiment was performed as three independent analyses.

4.8. RNA-seq data analysis

RNA-seq data of the adult tissues were obtained previously [10]. The reads were mapped to the *Ciona* genome (KY21 Gene Model) [63], using HISAT2 (version 2.1.0) [64] and quantified using RSEM (version 1.3.3) [65]. The resulting gene expression levels are presented as exported values of transcript per million (TPM).

4.9. RNA purification and qRT-PCR

Adult ascidian tissues (oral siphon, atrial siphon, neural complex, endostyle, heart, ovary, pharynx, stomach, and intestine) were collected as previously [10]. Total RNA from adult tissues and hemocytes was extracted, purified, and depleted of genomic DNA as previously [10]. An aliquot of 1 mg (for tissues) or 200 ng (for hemocytes) of DNase-treated total RNA was used for first-strand cDNA synthesis. qRT-PCR was performed using a CFX96 Real-time System and SsoAdvanced™ Universal SYBR Green Supermix (Bio-Rad Laboratories, Hercules, CA, USA). The primers are listed in Table S3. Gene expression levels were normalized to the reference genes: KY21.Chr10.446 for Figure 6 [10]; KY21.Chr9.158 (KH.C9.410) for Figure 8A [21]; and KY21.Chr2.148 for Figure 9. The KY21.Chr2.148 was identified by RNA-seq below to be constantly expressed following CiEMa stimulation. Given that the expression of the AMP genes at 0 hour varied among the data sets, the expression levels were normalized to the 0-hour values and set as 1. Three to four independent sets of samples were examined.

4.10. LPS stimulation

Hemocytes were collected from 2-3 ascidians as described above, and the cell number was quantified using a CDA-1000 particle counter (Sysmex Corporation, Hyogo, Japan). Cells were seeded at 1×10^6 - 2×10^6/well in a 24-well plate in medium consisting of sterile seawater (Nazeme 800; Japan QCE, Numazu, Japan) containing 20% hemolymph and 0.5× penicillin and streptomycin (Nacalai Tesque, Inc.). The plates were incubated for 16 hours at 18 °C. The hemocytes then were stimulated without or with LPS from *E. coli* 055:B5 (0.1 mg/mL, Millipore/Sigma–Aldrich, St. Louis, MO, USA) for 1, 2, and 4 hours at 18 °C. Four to six independent sets of the hemocytes (1 hour) and culture supernatants (1, 2, and 4 hours) were collected and used for qRT-PCR and dot blot analyses, respectively.

4.11. Dot blot analyses

The culture supernatants of hemocytes (incubatied with or without LPS for 1, 2, and 4 hours) were loaded onto a Sep-Pak C18 1 cc Vac Cartridge (Waters Corporation, Milford, MA, USA), washed with 10% acetonitrile, and eluted with 30% acetonitrile containing 0.1% TFA. For each sample, the eluent was dried using a Speed-Vac and dissolved in 10 mL of water. 1 mL of each sample was spotted onto a nitrocellulose membrane. The membrane was dried for 30 min at 100 °C, then blocked for 30 min with Block Ace (KAC Co., Ltd., Kyoto, Japan) in TBS containing 0.05% Tween 20 (TBST). The membrane was incubated with the affinity-purified anti-CiEMa antibody (1:2000), followed by the HRP-conjugated anti-rabbit IgG secondary antibody (1:2000, GE Healthcare, Buckinghamshire, UK). Signals were developed using an ECL substrate (GE Healthcare). Six different sets of samples were analyzed. Signals were captured using an Amersham™ Imager 600 (GE Healthcare) and then quantified using Fiji software [66]. The signals of pre-absorbed control were subtracted for CiEMa quantification.

4.12. CiEMa stimulation and RNA-sequencing

The isolated pharynx was incubated with 1 mM synthetic CiEMa in sterile seawater (Nazeme 800) containing 0.5×penicillin and streptomycin (Nacalai Tesque, Inc.) for 0, 1, 2, 4, and 8 hours at 18 °C. Total RNA was extracted, purified, and depleted of genomic DNA as described above. One and four sets of samples were collected and used for RNA-seq and qRT-PCR, respectively. An aliquot (500 ng) of quality-confirmed RNA was used for library construction and sequenced at Novagene (Beijing, China) using the Illumina NovaSeq 6000 platform. The resulting fastq files were analyzed as described above. The expression level (TPM) of each gene is listed in Table S2. The fastq files have been deposited in the NCBI database (Accession No. PRJNA1045840). The RNA-seq data were confirmed by qRT-PCR as described above.

4.13. Statistical analysis

Statistical analyses were performed using R software (version 4.2.2) as previously described [10]. In brief, the Levene test was initially performed to confirm the equal variance of expression level in each tissue (Figure 6B). Subsequently, the data were analyzed by a parametric one-way Analysis of Variance (ANOVA) with post hoc Tukey's multiple comparison tests (Figure 6B). For Figures 8 and 9, comparisons were conducted using a non-paired Student's *t*-test and one-way ANOVA, respectively. Note that, in Figure 9, the one-way ANOVA for each AMP gene was performed while excluding data from the 0-hour time point. Where applicable, analyses were performed as two-tailed tests. $P < 0.05$ was considered statistically significant. *P*-values for the Levene test, ANOVA, and Student's *t*-test are indicated as P_L, P_A, and P, respectively.

Supplementary Materials: The following supporting information can be downloaded at the website of this paper posted on Preprints.org. **Figure S1**: Original images of dot blot analyses in Figure 8B. Six independent data sets using anti-CiEMa antibody and pre-absorbed controls are shown.; **Table S1**: Quantification of dot blot analyses in Figure 8B.; **Table S2**: Raw TPM values of each gene by RNA-seq analyses.; **Table S3**: Primers for qRT-PCR.

Author Contributions: S. M. designed the experiments. S. M., R. I., M. O., H. N., T. R. K., A. S., T. O., T. K., and H. S. performed the experiments, analyzed the data, and wrote the paper.

Data Availability Statement: The fastq files have been deposited in the NCBI database (PRJNA1045840).

Acknowledgments: We thank Dr. Yutaka Satou, Dr. Manabu Yoshida, and all members of the Department of Zoology of Kyoto University; the Maizuru Fishery Research Station at Kyoto University; the Misaki Marine Biological Station at the University of Tokyo; and the National BioResource Project (NBRP) for cultivating and providing ascidians. We are also grateful to Dr. Fumihiko Sato for valuable comments and discussions regarding the manuscript. This work was supported, in part, by grants to S. M. (JP19K16182 and JP22K06307) from the Japan Society for the Promotion of Science (JSPS).

Conflicts of Interest: The authors declare no conflict of interest. The funders had no role in the design of the study; in the collection, analyses, or interpretation of data; in the writing of the manuscript; or in the decision to publish the results.

References

1. Buchmann, K. Evolution of Innate Immunity: Clues from Invertebrates via Fish to Mammals. *Front. Immunol.* **2014**, *5*, 459.
2. Yao, S.; Chan, J.; Xu, Y.; Wu, S.; Zhang, L. Divergences of the RLR Gene Families across Lophotrochozoans: Domain Grafting, Exon-Intron Structure, Expression, and Positive Selection. *Int. J. Mol. Sci.* **2022**, *23*, 3415.
3. Rast, J. P.; Smith, L. C.; Loza-Coll, M.; Hibino, T.; Litman, G. W. Genomic insights into the immune system of the sea urchin. *Science* **2006**, *314*, 952-956.
4. Huang, S.; Yuan, S.; Guo, L.; Yu, Y.; Li, J.; Wu, T.; Liu, T.; Yang, M.; Wu, K.; Liu, H.; et al. Genomic analysis of the immune gene repertoire of amphioxus reveals extraordinary innate complexity and diversity. *Genome Res.* **2008**, *18*, 1112-1126.
5. Zhang, L.; Li, L.; Guo, X.; Litman, G. W.; Dishaw, L. J.; Zhang, G. Massive expansion and functional divergence of innate immune genes in a protostome. *Sci. Rep.* **2015**, *5*, 8693.
6. Delsuc, F.; Brinkmann, H.; Chourrout, D.; Philippe, H. Tunicates and not cephalochordates are the closest living relatives of vertebrates. *Nature* **2006**, *439*, 965-968.
7. Satoh, N.; Rokhsar, D.; Nishikawa, T. Chordate evolution and the three-phylum system. *Proc. Biol. Sci.* **2014**, *281*, 20141729.
8. Lemaire, P. Evolutionary crossroads in developmental biology: the tunicates. *Development* **2011**, *138*, 2143-2152.
9. Satoh, N. The ascidian tadpole larva: comparative molecular development and genomics. *Nat. Rev. Genet.* **2003**, *4*, 285-295.
10. Matsubara, S.; Osugi, T.; Shiraishi, A.; Wada, A.; Satake, H. Comparative analysis of transcriptomic profiles among ascidians, zebrafish, and mice: Insights from tissue-specific gene expression. *PLoS ONE* **2021**, *16*, e0254308.
11. Satake, H.; Matsubara, S.; Shiraishi, A.; Yamamoto, T.; Osugi, T.; Sakai, T.; Kawada, T. Peptide receptors and immune-related proteins expressed in the digestive system of a urochordate, *Ciona intestinalis*. *Cell Tissue Res.* **2019**, *377*, 293-308.
12. Liberti, A.; Natarajan, O.; Atkinson, C. G. F.; Sordino, P.; Dishaw, L. J. Reflections on the Use of an Invertebrate Chordate Model System for Studies of Gut Microbial Immune Interactions. *Front. Immunol.* **2021**, *12*, 642687.
13. Longo, V.; Parrinello, D.; Longo, A.; Parisi, M. G.; Parrinello, N.; Colombo, P.; Cammarata, M. The conservation and diversity of ascidian cells and molecules involved in the inflammatory reaction: The *Ciona robusta* model. *Fish Shellfish Immunol.* **2021**, *119*, 384-396.
14. Franchi, N.; Ballarin, L. Immunity in Protochordates: The Tunicate Perspective. *Front. Immunol.* **2017**, *8*, 674.
15. Parrinello, N.; Cammarata, M.; Parrinello, D. The Inflammatory Response of Urochordata: The Basic Process of the Ascidians' Innate Immunity. In *Advances in Comparative Immunology*, Cooper, E., Eds.; Springer Cham, Switzerland, **2018**, pp. 521-590.
16. Satou, Y.; Nakamura, R.; Yu, D.; Yoshida, R.; Hamada, M.; Fujie, M.; Hisata, K.; Takeda, H.; Satoh, N. A Nearly Complete Genome of *Ciona intestinalis* Type A (*C. robusta*) Reveals the Contribution of Inversion to Chromosomal Evolution in the Genus *Ciona*. *Genome Biol. Evol.* **2019**, *11*, 3144-3157.
17. Dehal, P.; Satou, Y.; Campbell, R. K.; Chapman, J.; Degnan, B.; De Tomaso, A.; Davidson, B.; Di Gregorio, A.; Gelpke, M.; Goodstein, D. M.; et al. The draft genome of *Ciona intestinalis*: insights into chordate and vertebrate origins. *Science* **2002**, *298*, 2157-2167.
18. Vizzini, A.; Bonura, A.; La Paglia, L.; Fiannaca, A.; La Rosa, M.; Urso, A.; Arizza, V. ceRNA Network Regulation of TGF-beta, WNT, FOXO, Hedgehog Pathways in the Pharynx of *Ciona robusta*. *Int. J. Mol. Sci.* **2021**, *22*, 3497.

19. Zhang, W.; Jiang, A.; Yu, H.; Dong, B. Comparative Transcriptomic Analysis Reveals the Functionally Segmented Intestine in Tunicate Ascidian. *Int. J. Mol. Sci.* **2023**, *24*, 6270.
20. Ogasawara, M.; Nakazawa, N.; Azumi, K.; Yamabe, E.; Satoh, N.; Satake, M. Identification of thirty-four transcripts expressed specifically in hemocytes of *Ciona intestinalis* and their expression profiles throughout the life cycle. *DNA Res.* **2006**, *13*, 25-35.
21. Ohtsuka, Y.; Inagaki, H. *In silico* identification and functional validation of linear cationic alpha-helical antimicrobial peptides in the ascidian *Ciona intestinalis*. *Sci. Rep.* **2020**, *10*, 12619.
22. Udit, S.; Blake, K.; Chiu, I. M. Somatosensory and autonomic neuronal regulation of the immune response. *Nat. Rev. Neurosci.* **2022**, *23*, 157-171.
23. Yang, D.; Biragyn, A.; Hoover, D. M.; Lubkowski, J.; Oppenheim, J. J. Multiple roles of antimicrobial defensins, cathelicidins, and eosinophil-derived neurotoxin in host defense. *Annu. Rev. Immunol.* **2004**, *22*, 181-215.
24. Kawada, T.; Ogasawara, M.; Sekiguchi, T.; Aoyama, M.; Hotta, K.; Oka, K.; Satake, H. Peptidomic analysis of the central nervous system of the protochordate, *Ciona intestinalis*: homologs and prototypes of vertebrate peptides and novel peptides. *Endocrinology* **2011**, *152*, 2416-2427.
25. Aoyama, M.; Kawada, T.; Fujie, M.; Hotta, K.; Sakai, T.; Sekiguchi, T.; Oka, K.; Satoh, N.; Satake, H. A novel biological role of tachykinins as an up-regulator of oocyte growth: identification of an evolutionary origin of tachykininergic functions in the ovary of the ascidian, *Ciona intestinalis*. *Endocrinology* **2008**, *149*, 4346-4356.
26. Aoyama, M.; Kawada, T.; Satake, H. Localization and enzymatic activity profiles of the proteases responsible for tachykinin-directed oocyte growth in the protochordate, *Ciona intestinalis*. *Peptides* **2012**, *34*, 186-192.
27. Matsubara, S.; Shiraishi, A.; Osugi, T.; Kawada, T.; Satake, H. The regulation of oocyte maturation and ovulation in the closest sister group of vertebrates. *eLife* **2019**, *8*, e49062.
28. Matsubara, S.; Shiraishi, A.; Osugi, T.; Kawada, T.; Satake, H. Fractionation of Ovarian Follicles and *in vitro* Oocyte Maturation and Ovulation Assay of *Ciona intestinalis* Type A. *Bio. Protoc.* **2020**, *10*, e3577.
29. Osugi, T.; Miyasaka, N.; Shiraishi, A.; Matsubara, S.; Satake, H. Cionin, a vertebrate cholecystokinin/gastrin homolog, induces ovulation in the ascidian *Ciona intestinalis* type A. *Sci. Rep.* **2021**, *11*, 10911.
30. Sakai, T.; Yamamoto, T.; Watanabe, T.; Hozumi, A.; Shiraishi, A.; Osugi, T.; Matsubara, S.; Kawada, T.; Sasakura, Y.; Takahashi, T.; et al. Characterization of a novel species-specific 51-amino acid peptide, PEP51, as a caspase-3/7 activator in ovarian follicles of the ascidian, *Ciona intestinalis* Type A. *Front. Endocrinol. (Lausanne)* **2023**, *14*, 1260600.
31. Fedders, H.; Michalek, M.; Grotzinger, J.; Leippe, M. An exceptional salt-tolerant antimicrobial peptide derived from a novel gene family of haemocytes of the marine invertebrate *Ciona intestinalis*. *Biochem. J.* **2008**, *416*, 65-75.
32. Fedders, H.; Leippe, M. A reverse search for antimicrobial peptides in *Ciona intestinalis*: identification of a gene family expressed in hemocytes and evaluation of activity. *Dev. Comp. Immunol.* **2008**, *32*, 286-298.
33. Vizzini, A.; Bonura, A.; Parrinello, D.; Sanfratello, M. A.; Longo, V.; Colombo, P. LPS challenge regulates gene expression and tissue localization of a *Ciona intestinalis* gene through an alternative polyadenylation mechanism. *PLoS ONE* **2013**, *8*, e63235.
34. Longo, V.; Longo, A.; Martorana, A.; Lauria, A.; Augello, G.; Azzolina, A.; Cervello, M.; Colombo, P. Identification of an LPS-Induced Chemo-Attractive Peptide from *Ciona robusta*. *Mar. Drugs* **2020**, *18*, 209.
35. Brozovic, M.; Dantec, C.; Dardaillon, J.; Dauga, D.; Faure, E.; Gineste, M.; Louis, A.; Naville, M.; Nitta, K. R.; Piette, J.; et al. ANISEED 2017: extending the integrated ascidian database to the exploration and evolutionary comparison of genome-scale datasets. *Nucleic Acids Res.* **2018**, *46*, D718-D725.
36. Osugi, T.; Sasakura, Y.; Satake, H. The ventral peptidergic system of the adult ascidian *Ciona robusta* (*Ciona intestinalis* Type A) insights from a transgenic animal model. *Sci. Rep.* **2020**, *10*, 1892.
37. Shida, K.; Terajima, D.; Uchino, R.; Ikawa, S.; Ikeda, M.; Asano, K.; Watanabe, T.; Azumi, K.; Nonaka, M.; Satou, Y.; et al. Hemocytes of *Ciona intestinalis* express multiple genes involved in innate immune host defense. *Biochem. Biophys. Res. Commun.* **2003**, *302*, 207-218.
38. Terajima, D.; Yamada, S.; Uchino, R.; Ikawa, S.; Ikeda, M.; Shida, K.; Arai, Y.; Wang, H. G.; Satoh, N.; Satake, M. Identification and sequence of seventy-nine new transcripts expressed in hemocytes of *Ciona intestinalis*, three of which may be involved in characteristic cell-cell communication. *DNA Res.* **2003**, *10*, 203-212.
39. Sasaki, N.; Ogasawara, M.; Sekiguchi, T.; Kusumoto, S.; Satake, H. Toll-like receptors of the ascidian *Ciona intestinalis*: prototypes with hybrid functionalities of vertebrate Toll-like receptors. *J. Biol. Chem.* **2009**, *284*, 27336-27343.
40. Chiba, S.; Sasaki, A.; Nakayama, A.; Takamura, K.; Satoh, N. Development of *Ciona intestinalis* juveniles (through 2nd ascidian stage). *Zoolog. Sci.* **2004**, *21*, 285-298.
41. Iguchi, R.; Nakayama, S.; Sasakura, Y.; Sekiguchi, T.; Ogasawara, M. Repetitive and zonal expression profiles of absorption-related genes in the gastrointestinal tract of ascidian *Ciona intestinalis* type A. *Cell Tissue Res.* **2023**, *394*, 343-360.

42. Liberti, A.; Melillo, D.; Zucchetti, I.; Natale, L.; Dishaw, L. J.; Litman, G. W.; De Santis, R.; Pinto, M. R. Expression of *Ciona intestinalis* variable region-containing chitin-binding proteins during development of the gastrointestinal tract and their role in host-microbe interactions. *PLoS ONE* **2014**, *9*, e94984.
43. Nakayama, S.; Ogasawara, M. Compartmentalized expression patterns of pancreatic- and gastric-related genes in the alimentary canal of the ascidian *Ciona intestinalis*: evolutionary insights into the functional regionality of the gastrointestinal tract in Olfactores. *Cell Tissue Res.* **2017**, *370*, 113-128.
44. Parrinello, N.; Vizzini, A.; Salerno, G.; Sanfratello, M. A.; Cammarata, M.; Arizza, V.; Vazzana, M.; Parrinello, D. Inflamed adult pharynx tissues and swimming larva of *Ciona intestinalis* share CiTNFalpha-producing cells. *Cell Tissue Res.* **2010**, *341*, 299-311.
45. Vizzini, A.; Di Falco, F.; Parrinello, D.; Sanfratello, M. A.; Mazzarella, C.; Parrinello, N.; Cammarata, M. *Ciona intestinalis* interleukin 17-like genes expression is upregulated by LPS challenge. *Dev. Comp. Immunol.* **2015**, *48*, 129-137.
46. Vizzini, A.; Di Falco, F.; Parrinello, D.; Sanfratello, M. A.; Cammarata, M. Transforming growth factor beta (CiTGF-beta) gene expression is induced in the inflammatory reaction of *Ciona intestinalis*. *Dev. Comp. Immunol.* **2016**, *55*, 102-110.
47. Shi, W.; Peyrot, S. M.; Munro, E.; Levine, M. FGF3 in the floor plate directs notochord convergent extension in the *Ciona* tadpole. *Development* **2009**, *136*, 23-28.
48. Ikuta, T.; Satoh, N.; Saiga, H. Limited functions of Hox genes in the larval development of the ascidian *Ciona intestinalis*. *Development* **2010**, *137*, 1505-1513.
49. Trivedi, S.; Ueki, T.; Yamaguchi, N.; Michibata, H. Novel vanadium-binding proteins (vanabins) identified in cDNA libraries and the genome of the ascidian *Ciona intestinalis*. *Biochim. Biophys. Acta* **2003**, *1630*, 64-70.
50. Yamaguchi, N.; Kamino, K.; Ueki, T.; Michibata, H. Expressed sequence tag analysis of vanadocytes in a vanadium-rich ascidian, *Ascidia sydneiensis samea*. *Mar. Biotechnol. (NY)* **2004**, *6*, 165-74.
51. Yamaguchi, N.; Amakawa, Y.; Yamada, H.; Ueki, T.; Michibata, H. Localization of vanabins, vanadium-binding proteins, in the blood cells of the vanadium-rich ascidian, *Ascidia sydneiensis samea*. *Zoolog. Sci.* **2006**, *23*, 909-15.
52. Di Bella, M. A.; Fedders, H.; De Leo, G.; Leippe, M. Localization of antimicrobial peptides in the tunic of *Ciona intestinalis* (Ascidiacea, Tunicata) and their involvement in local inflammatory-like reactions. *Results. Immunol.* **2011**, *1*, 70-75.
53. Vizzini, A.; Parrinello, D.; Sanfratello, M. A.; Salerno, G.; Cammarata, M.; Parrinello, N. Inducible galectins are expressed in the inflamed pharynx of the ascidian *Ciona intestinalis*. *Fish Shellfish Immunol.* **2012**, *32*, 101-109.
54. Hatakeyama, T.; Unno, H. Functional Diversity of Novel Lectins with Unique Structural Features in Marine Animals. *Cells* **2023**, *12*, 1814.
55. Otero-Gonzalez, A. J.; Magalhaes, B. S.; Garcia-Villarino, M.; Lopez-Abarrategui, C.; Sousa, D. A.; Dias, S. C.; Franco, O. L. Antimicrobial peptides from marine invertebrates as a new frontier for microbial infection control. *FASEB J* **2010**, *24*, 1320-1334.
56. Canesi, L.; Auguste, M.; Balbi, T.; Prochazkova, P. Soluble mediators of innate immunity in annelids and bivalve mollusks: A mini-review. *Front. Immunol.* **2022**, *13*, 1051155.
57. Darmer, D.; Schmutzler, C.; Diekhoff, D.; Grimmelikhuijzen, C. J., Primary structure of the precursor for the sea anemone neuropeptide Antho-RFamide (less than Glu-Gly-Arg-Phe-NH2). *Proc. Natl. Acad. Sci. USA.* **1991**, *88*, 2555-2559.
58. Schmutzler, C.; Diekhoff, D.; Grimmelikhuijzen, C. J. The primary structure of the Pol-RFamide neuropeptide precursor protein from the hydromedusa *Polyorchis penicillatus* indicates a novel processing proteinase activity. *Biochem. J.* **1994**, *299*, 431-436.
59. Schmutzler, C.; Darmer, D.; Diekhoff, D.; Grimmelikhuijzen, C. J. Identification of a novel type of processing sites in the precursor for the sea anemone neuropeptide Antho-RFamide (<Glu-Gly-Arg-Phe-NH2) from *Anthopleura elegantissima*. *J. Biol. Chem.* **1992**, *267*, 22534-22541.
60. Takahashi, T. Neuropeptides and epitheliopeptides: structural and functional diversity in an ancestral metazoan Hydra. *Protein Pept. Lett.* **2013**, *20*, 671-680.
61. Satou, Y.; Kawashima, T.; Shoguchi, E.; Nakayama, A.; Satoh, N. An integrated database of the ascidian, *Ciona intestinalis*: towards functional genomics. *Zoolog. Sci.* **2005**, *22*, 837-843.
62. Parrinello, D.; Parisi, M.; Parrinello, N.; Cammarata, M. *Ciona robusta* hemocyte populational dynamics and PO-dependent cytotoxic activity. *Dev. Comp. Immunol.* **2020**, *103*, 103519.
63. Satou, Y.; Tokuoka, M.; Oda-Ishii, I.; Tokuhiro, S.; Ishida, T.; Liu, B.; Iwamura, Y. A Manually Curated Gene Model Set for an Ascidian, *Ciona robusta* (*Ciona intestinalis* Type A). *Zoolog. Sci.* **2022**, *39*, 253-260.
64. Kim, D.; Paggi, J. M.; Park, C.; Bennett, C.; Salzberg, S. L. Graph-based genome alignment and genotyping with HISAT2 and HISAT-genotype. *Nat. Biotechnol.* **2019**, *37*, 907-915.

65. Li, B.; Dewey, C. N. RSEM: accurate transcript quantification from RNA-Seq data with or without a reference genome. *BMC Bioinformatics* **2011**, *12*, 323.
66. Schindelin, J.; Arganda-Carreras, I.; Frise, E.; Kaynig, V.; Longair, M.; Pietzsch, T.; Preibisch, S.; Rueden, C.; Saalfeld, S.; Schmid, B.; et al. Fiji: an open-source platform for biological-image analysis. *Nat. Methods* **2012**, *9*, 676-682.